REVIEW

https://doi.org/10.1038/s41586-019-1643-z

Subducting carbon

Terry Plank[1]* & Craig E. Manning[2]

A hidden carbon cycle exists inside Earth. Every year, megatons of carbon disappear into subduction zones, affecting atmospheric carbon dioxide and oxygen over Earth's history. Here we discuss the processes that move carbon towards subduction zones and transform it into fluids, magmas, volcanic gases and diamonds. The carbon dioxide emitted from arc volcanoes is largely recycled from subducted microfossils, organic remains and carbonate precipitates. The type of carbon input and the efficiency with which carbon is remobilized in the subduction zone vary greatly around the globe, with every convergent margin providing a natural laboratory for tracing subducting carbon.

In addition to its familiar cycling between the terrestrial biosphere and atmosphere, carbon moves from microfossils on the seafloor to erupting volcanoes and deep diamonds, in a cycle driven by plate tectonics. Subduction links surface biological processes with the deep Earth, creating a planet suffused with the signature of life. The fate and flux of carbon vary from trench to trench, as every subducting slab delivers to the mantle a singular mix of organic and inorganic carbon that heats and pressurizes at a particular rate determined by its age and convergence speed. The inherent reactivity of carbon in each input package and the pressure–temperature–time path experienced by each slab drive chemical reactions that separate carbon into two parts: one that is carried deeper into Earth and one that returns to the surface. Here we discuss (I) the geological happenstance that delivers carbon to deep sea trenches today, (II) the reactions and movements in the subduction zone that mobilize carbon into fluids and melts, (III) the carbon that continues deep into the mantle to form molten carbonates and diamonds, and (IV) the carbon that escapes such a deep descent to be eventually emitted from arc volcanoes (Fig. 1).

Although excellent reviews exist on the global consequence of the deep carbon cycle over Earth's history[1–6], our focus here is on the variability in current subduction systems, where carbon inputs and outputs can reveal the physicochemical processes occurring in the subduction zone that ultimately drive the directionality of the cycle. We highlight end-member subduction zones with distinct inputs or pathways, such as Tonga (little sedimentary carbon) and Cascadia (hot slab), each presenting a different natural recycling experiment worthy of focused study. We also show how recent advances in both laboratory and computational approaches now lead to predictions of how and when carbon mobilizes into upward-moving fluids or remains in solid form in the downgoing plate. Finally, we present recent evidence from satellites, portable instruments and melt inclusions that suggests that most of the carbon in arc magmas is recycled from the subduction zone.

The global carbon flux perspective

Earth exhales carbon at volcanoes. Current estimates place the total volcanic outgassing rate at 79 ± 9 (uncertainty 1σ) megatons of carbon per year (Mt C yr^{-1}), with similar amounts emitted at mid-ocean ridges and subduction zones, and the greatest quantities emitted diffusely in intraplate volcanic regions (Box 1). Uncertainties in estimates of volcanic emission rates are quickly declining owing to long-term satellite observation[7] and direct sampling of volcanic plumes and diffuse emanations[8–10]. The spatial variability in volcanic carbon is enormous, however, and currently six volcanoes are estimated to control the global budget of direct emissions (Nyiragongo, Popocateptl, Etna, Ambrym, Bagana and Aoba; together contributing more than 5 Mt C yr^{-1})[11]. The largest volcanic emissions, however, may be emanating diffusely from calderas and faults[10]. Although current anthropogenic fluxes (about 9,500 Mt C yr^{-1})[12] dwarf volcanic ones, the long-term fluxes of carbon to the atmosphere have been dominated by volcanic sources over most of Earth's history. The rate of supply of mantle carbon is governed by tectonic rates of plate spreading and convergence, as well as the plume flux from the deeper mantle, punctuated by large igneous provinces that supply bursts of CO_2 in short periods of time.

Deep-Earth carbon fluxes are not a one-way street, however. There is an equally substantial, highly uncertain and spatially variable carbon flux that enters the mantle with oceanic plates at subducting zones. This carbon is derived largely from the ocean, in the form of carbonate shells and remains of marine organisms, as well as carbonate in the oceanic lithosphere. Terrestrial organic carbon is also washed onto the seafloor by large rivers. The fate of subducting carbon has a profound effect on Earth's evolution, and depends on the efficiency with which carbon is returned to Earth's surface by devolatilization reactions in the subducting slab and by upward transport in magmas that supply volcanic arcs. We will refer to this return flux of carbon to Earth's surface as 'recycling'. A recycling efficiency of 0% means that none of the carbon that is subducted returns to Earth's surface, but instead is sequestered in the mantle for geologically significant durations.

A low recycling efficiency could have planetary consequences. For example, Earth's surface has a distinctively high H/C ratio, about an order of magnitude higher than Earth's chondritic building blocks[13]. Is this due to more efficient subduction recycling of H_2O than that of C over Earth's history[4]? The deep subduction of reduced organic carbon amounts to a loss of electrons and therefore an increase in the oxidative potential of Earth's surface[1]. Has a low recycling efficiency of organic carbon contributed to Earth's oxygen-rich surface[14]? Or is the oxidation of the mantle the net effect of subduction[15], given the higher input flux of carbonate than that of organic carbon? What is the separate fate of these oxidized and reduced forms of carbon?

A high recycling efficiency creates a direct connection between subducting carbon and CO_2 supply to the atmosphere. For example, there may have been greater subduction of carbonate at certain times in Earth's history, such as the Mesozoic era, when the seafloor of the shallow Tethys ocean subducted. Did this lead to higher volcanic CO_2

[1]Lamont-Doherty Earth Observatory, Columbia University, Palisades, NY, USA. [2]University of California, Los Angeles, CA, USA. *e-mail: tplank@ldeo.columbia.edu

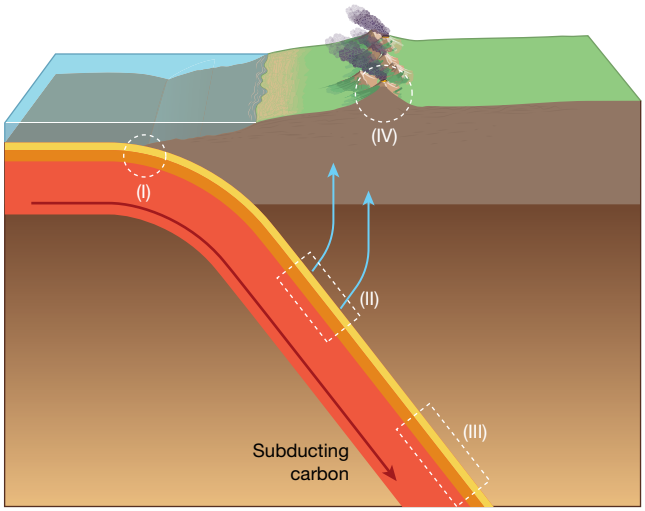

Fig. 1 | The deep carbon cycle. (I) Carbon input to subduction zones from the sedimentary (yellow), oceanic crust (orange) and mantle (red) layers in the downgoing plate (dark red arrow). (II) Decarbonation reactions in the subduction zone release carbon to upward-moving fluids and melts (blue arrows). (III) Deeply subducted carbon, potentially forming diamonds. (IV) Emission of recycled carbon to the surface via arc volcanism.

emissions and therefore greater warming[16,17]? Does the climate system respond to CO_2 precipitation in the oceanic crust as a sink or source of carbon, and how is this process modulated by plate spreading rates, ocean bottom temperatures and subduction delivery[18,19]? What are the long-term climate consequences of the fact that subduction of carbonate is a relatively recent development, tied to evolution of calcifying marine microorganisms[20]? Participation of carbonate subduction in the deep carbon cycle is arguably a recent phenomenon[5].

It is therefore critical to understand the efficiency of carbon subduction recycling, which is determined by two general approaches. One is to balance the input (subducted) and output (arc volcanic) fluxes of carbon globally[2,3]. The most recent estimates indicate about 30% recycling, although the uncertainties are very large in several fluxes (Box 1). Weak correlations may exist between decarbonation efficiency and slab age[21]. The other approach is to characterize the physicochemical processes in subduction zones that drive recycling, such as fluid and melt generation and transport, coupled with carbon solubility and reaction kinetics, given different carbon feedstocks and pressure–temperature paths. Here we focus on the latter approach and trace carbon through the recycling process, first by considering how and when carbon is deposited on and precipitated in subducting seafloor.

Subducting carbon

Although the ocean is full of carbon—dissolved as bicarbonate and in the shells and bodies of marine organisms—very little carbon makes it to the deep seafloor to be conveyed to a trench. The carbon that enters subduction zones includes calcium carbonate and reduced organic carbon that exist within the sedimentary, oceanic crust and mantle layers of the incoming plate. Each trench makes unique selections from the carbon menu.

Starting with the lowermost layer, mantle peridotite that forms the bulk of the subducting lithosphere readily hydrates and carbonates if exposed to seawater, forming carbonated serpentinites[22]. However, most peridotite usually resides at least 6 km beneath the seafloor and is not in direct contact with seawater. Faulting and fracturing are necessary to bring mantle rocks to the sea floor or seawater to the mantle. Carbonated serpentinites may form near spreading centres or near trenches. Near spreading centres, extensional faulting is linked to hydration and carbonation reactions, as well as to the precipitation of magnesium and calcium carbonate veins in mantle peridotites[22]. Carbon isotopes in oceanic peridotites reflect mixing between seawater-derived carbonate and reduced carbon[23]. Serpentinization is most pronounced at slow-spreading mid-ocean ridges, but most subducting lithosphere is not formed there, because of the low plate production rate and the preferential existence of subduction zones and fast-spreading crust in the Pacific. Oceanic carbonated serpentinites therefore make a minor contribution to the global carbon input flux to subduction zones[3], although they may be locally important. The volcanism at the South Sandwich margin, where slow-spreading crust is preferentially consumed, is notable for having some of the highest $^{11}B/^{10}B$ ratios among island arcs, a feature that could be derived from the high $^{11}B/^{10}B$ ratio that is typical of seafloor serpentinized peridotites[24]. The South Sandwich margin may thus represent a rare case, in which subducting carbon predominantly resides in oceanic carbonated serpentinite (Box 2).

Near trenches, the subducting plate deforms and fractures because of bending. The resulting faults have been seismically imaged to penetrate into the mantle of the incoming plate, and seismic velocities decrease towards the trench[25], leading to speculation that the extent of hydration due to ingress of seawater could consume an ocean every billion years[26,27]. However, outer-rise serpentinites have never been sampled, and other factors besides hydration—such as fracturing and anisotropy—may explain this reduction in seismic velocity. The extent of carbonation in unsampled outer-rise serpentinites is also unknown, and fluid pathways longer than 5 km may lead to low fluid-to-rock ratios and low carbon transport into the mantle section of the downgoing plate[23]. Indeed, electrical-resistivity imaging does not support extensive reaction of seawater with the mantle section of the incoming plate at the Central America trench[28]. Most global flux estimates for carbonated peridotite are low (Box 1).

In contrast to peridotite carbonation, there is abundant evidence for pervasive carbonation of the near-ridge oceanic crust. Seawater-derived fluids circulate predominantly in the higher-permeability upper-crustal volcanic section, leading to low-temperature precipitation of carbonate minerals. Because these carbonates are largely seawater-derived, they are isotopically heavy ($\delta^{13}C \approx 0‰$, where $\delta^{13}C$ is the deviation of the ratio $^{13}C/^{12}C$ relative to that of Pee Dee belemnite), although some biotic and abiotic processes also lead to CO_2 reduction and precipitation of isotopically light carbon ($\delta^{13}C < -20‰$[29,30]; Fig. 2a). Nonetheless, the dominant form of carbon in altered oceanic crust (AOC) is calcium carbonate (calcite and aragonite) that precipitates in veins and vugs, as has been found in samples from a small number (about 15) of drill sites. Carbon uptake occurs near the ridge axis in crust that is 20 Myr old, but surprisingly, AOC older than 80 Myr has higher carbonate content[31]. This may be due to higher bottom-water temperatures in the Cretaceous period promoting greater abiogenic carbonate precipitation[32]. Although low in carbonate, young AOC (less than 10 Myr old) is isotopically light owing to the intense bio-alteration of young crust[30]. Thus, an important prediction for carbon inputs is that old plates (for example, Marianas and Tonga) will have greater AOC carbonate concentrations and higher average $\delta^{13}C$, whereas young plates (for example, Cascadia and Central America) will have little AOC carbonate with lower $\delta^{13}C$ (Fig. 2a).

The sedimentary layer that is deposited on top of the oceanic crust contains dramatically different forms of carbon than the largely inorganic precipitates of the oceanic crust and peridotite. Sediments are the graveyard of marine organisms and the resting place of terrestrial organic remains. Organisms that grow a carbonate shell, such as nannoplankton coccoliths and bottom-dwelling foraminifera, are the richest source of carbon deposits on the seafloor. For example, a 100-m section of nannofossil ooze may contain as much carbon as the entire oceanic crust below it (using average values given in ref. [3]). Marine sediments also contain the organic remains of marine and terrestrial organisms. Although most sediments have less than 1 wt% organic carbon, deep-sea fans can dominate the input flux at some margins. For example, a 1.5-km section of terrigenous turbidites with 0.35 wt% organic C (Fig. 2a) contains more carbon than the average oceanic crust. The balance of marine carbonate ($\delta^{13}C = 0‰$ to $+3‰$) versus organic carbon ($\delta^{13}C = -22‰$ to $-27‰$) has a very large effect on

the isotopic composition of subducting carbon (see ref. [33] and Fig. 2a). Carbonate sediments can approach 100% $CaCO_3$ and therefore may contain more than 10 times the carbon of a sediment rich in organic carbon (1% C; Fig. 2a). This is offset by a greater flux of organic carbon-bearing sediments approaching trenches (in thick fans), so the proportion of organic to inorganic carbon subducted globally may be about 20% (ref. [34]).

Although sedimentary carbon has the potential to dominate global input fluxes, it may be entirely absent from some subducting sections. Indeed, the odds are stacked against carbon burial, as most carbonate dissolves and organic carbon oxidizes in the water column before reaching the seafloor. The ocean's cold and corrosive bottom waters are particularly challenging to carbonate survival. The calcite compensation depth (CCD), which marks the transition between carbonate-bearing and carbonate-absent sediments, is about 5,000 m deep in today's oceans. The CCD increases locally if the carbonate flux is high, as occurs in regions of high biological productivity, but it was generally shallower (less than 3,500 m) earlier in the Cenozoic era[35] and the Cretaceous period[36]. Much of the oceanic crust subducting today is old (average age of about 70 Myr)[37] and the combination of a shallower CCD and thermal subsidence with age means that carbonate is rare on the seafloor near trenches. For example, essentially zero sedimentary carbonate is subducted along the Tonga, Central Aleutian and Kuriles–Kamchatka trenches. On the other hand, abundant carbonate is subducted at the Central American margin, where the seafloor is beneath regions of high biological productivity, and at the New Zealand margin, where the seafloor is shallow[38] (Box 2).

Organic carbon is also consumed in the oxic ocean and in the sediments themselves by microbially mediated reactions, so its preservation in sediments requires rapid supply and burial. These conditions are met beneath regions of high biological productivity and in deep-sea fans, where rivers deliver high fluxes of carbon-bearing sediment to the ocean from regions of active uplift and erosion[39]. On the other hand, vast expanses of the ocean are deserts owing to low biological productivity and to the challenge of survival in the harsh oxic sediments[40]. Seafloor currently subducting in the western Pacific spent most of its lifetime traversing the central gyres and is therefore devoid of organic carbon; essentially no organic carbon is subducted at Tonga or Honshu[34]. By contrast, turbidite sediments in the Bengal and Indus fans, which derive from and fringe India's collision zone with Asia, constitute the largest fluxes of organic carbon into trenches. Other margins with notable piles of sediment containing organic carbon include those of Nankai, Cascadia, Alaska, South Chile and the Southern Antilles[34].

Thus, subducting carbon depends on geologic happenstance at locations where a deep-sea fan (high sedimentary organic carbon) or shallow seafloor (high sedimentary carbonate) happen to be near a trench, or where the subducting oceanic plate happens to be created by slow spreading (favouring carbonated serpentinites) or was formed in the Cretaceous period (favouring carbonated oceanic crust). There is exceptionally wide global variation in carbon input to a subduction zone; each downgoing plate has a distinct formation, evolution and sedimentation history (Box 2 and ref. [5]), with potentially large along-strike variations[41]. Global averaging obscures these underlying factors controlling recycling efficiency, which are essential for constructing the long-term history of the deep carbon cycle. This affects not only the amount and distribution of subducting carbon but also its reactivity and isotopic composition, and contributes to heterogeneity in the deep Earth. The former affects the fate of carbon in the subduction zone (discussed in the next section) and the latter serves as a useful tracer for the source of volcanic gases and diamonds (discussed in subsequent sections).

Reactions in subducting carbon

Once subducting lithosphere and sediment, and the carbon that they carry, are transported beyond the trench (point (I) in Fig. 1), the fate of carbon is determined by a game of subtraction. Rising pressure and temperature transform the subducted materials chemically and

Box 1

Global carbon flux into and out of the mantle

Following the work of Kelemen & Manning[3], several studies have investigated carbon fluxes as part of the Deep Carbon Observatory programme. On the input side, carbon concentration and isotope measurements[30] of AOC have yielded a slightly lower flux (18 Mt C yr^{-1}) than that reported in ref. [3] (25 Mt C yr^{-1}). Nonetheless, bulk AOC carbon estimates have remained consistent at 400–600 ppm C (refs. [102,105]). Two recent studies[34,106] have revised the C flux in subducting sediments substantially upwards compared to ref. [3] (13–23 Mt C yr^{-1} according to ref. [38]). One estimate (~60 Mt C yr^{-1}) includes 20% organic carbon[34] and another (57 Mt C yr^{-1}) is based on a model of the calcite compensation depth[106]. Both ref. [3] (10 Mt C yr^{-1}) and ref. [23] (1.3 Mt C yr^{-1}) estimate low C fluxes in subducting peridotite.

On the output side, identical MORB C fluxes (16 Mt C yr^{-1}) are derived from C in vapour-undersaturated volcanic glasses[93] and a coupled degassing model for C and noble gases[107]. The C flux estimates for actively degassing arcs and intraplate volcanoes[10] are immensely improved owing to satellite estimates of S fluxes[7], coupled with recent measurements of the CO_2/S ratio in volcanic gases[11]. Considerable diffuse degassing is associated predominantly with intraplate calderas and geothermal systems[10].

On balance, estimates of C input and output fluxes are remarkably similar, although uncertainties are large especially for subducting sedimentary C fluxes. Arc outputs currently represent 27^{+23}_{-16}% of the inputs (based on a Monte Carlo propagation of 2σ uncertainties), roughly half of that derived from the averages in ref. [3]. This reflects both increases in the sediment input and decreases in the arc output fluxes estimated in recent studies.

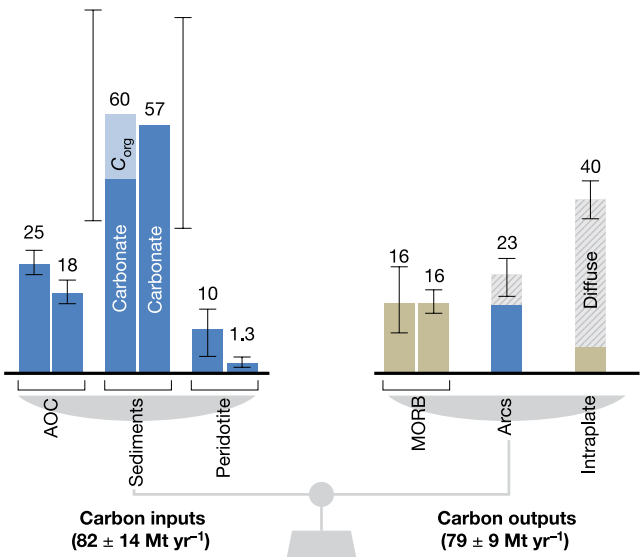

Box 1 Fig. 1 | Carbon flux balance for inputs to and outputs from the mantle. All values shown are in megatons per year. Dark blue boxes are specific to subduction zones. Diagonal ruling denotes diffuse degassing. Error bars are 1σ, as quoted or estimated by individual studies. The total input and output fluxes include 1σ uncertainties calculated by Monte Carlo propagation, but are probably underestimates, given the lack of information on the distribution of values or sources of uncertainties in most studies.

Box 2

Roadmap to carbon subduction and recycling

Each subduction zone is fed by a different feedstock of carbon contained within sediments, oceanic crust and serpentinized mantle of the incoming plate. Sediments may host both organic carbon and carbonate. The subduction zones highlighted in Box 2 Fig. 1 are dominated by one kind of carbon feedstock, and so can serve as sites for natural recycling experiments to determine the downstream fate of different kinds of input. For example, because little sedimentary carbon is subducted at Tonga, AOC carbon recycling can be isolated in the context of cold subduction.

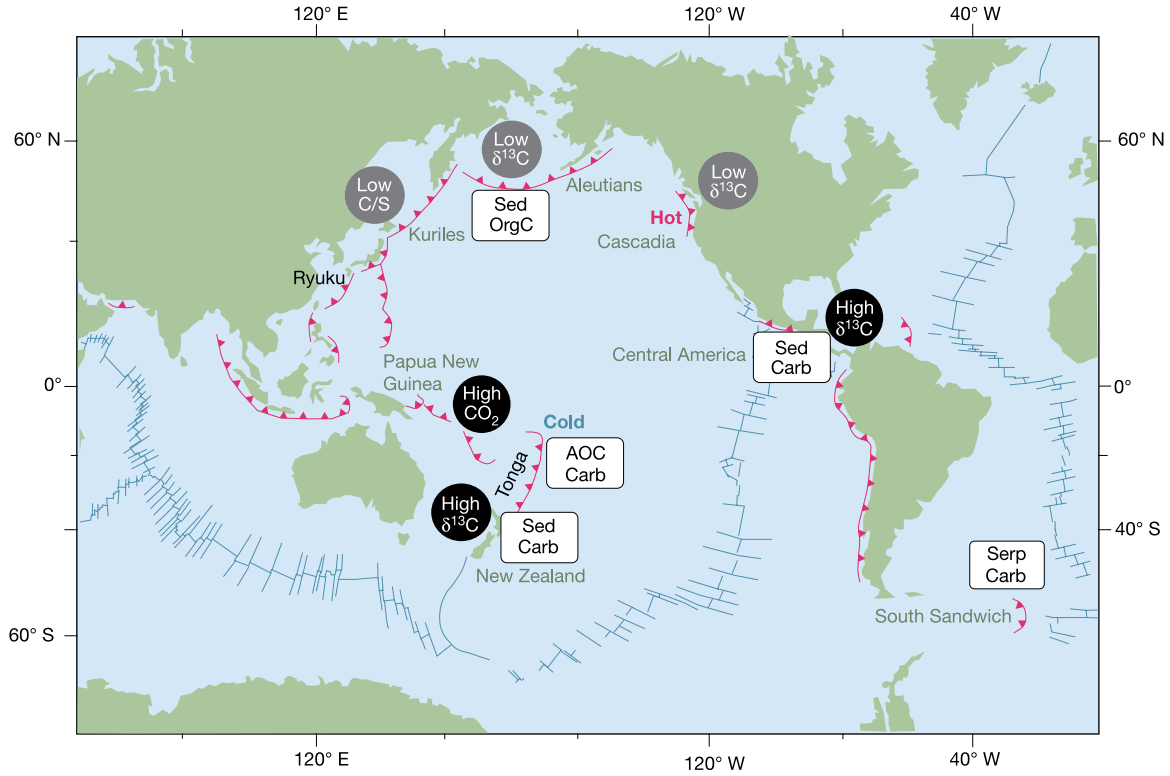

Box 2 Fig. 1 | Map of subduction systems that isolate different carbon inputs. Carb, carbonate; OrgC, organic carbon; Sed, sediment; Serp, serpentinite; C/S, CO_2/S ratio.

Box 2 Table | Attributes of each highlighted subduction zone

Subduction zone	Attribute	Notes	References
South Sandwich	Carbonated serpentinite	Very slow-spreading crust	97
Central America	Carbonate sediments	High biological productivity; high C_{org}	34,38
	High $\delta^{13}C$ in arc	Mean $\delta^{13}C$ of −3.0‰	92
Cascadia	Hot slab	Young subducting plate	98
	Low $\delta^{13}C$ in arc	Mean $\delta^{13}C$ of −8.6‰	92
Aleutians	High C_{org} in turbidites	Little carbonate	34,38
	Low $\delta^{13}C$ in arc	Mean $\delta^{13}C$ of −7.0‰	92
Honshu–Kuriles	Low CO_2/S in arc	Little sedimentary C	34,89
Papua New Guinea–Vanuatu	High CO_2 flux in arc	Subducting carbonate	11
Tonga	AOC carbon, cold slab	Little carbon in sediments	32,38
New Zealand	Carbonate sediments	Shallow seafloor	34,38
	High $\delta^{13}C$ in arc	Mean $\delta^{13}C$ of −3.0‰	92

physically, setting the stage for fractional carbon removal by a mix of processes that determine recycling efficiency.

During transit to sub-arc depths, three main processes subtract carbon from the slab: mechanical removal, metamorphic decarbonation and melting (Box 3). Frontal accretion or underplating of sediment during the initial stages of subduction may remove a substantial amount of carbon[41]. The dynamic environment at the top of the slab can result in mixing and removal of slab material. Complex tectonic mixtures of lithologies—mélanges—are important in many exhumed subduction complexes, but to first order they are subject to the same set of processes as their constituent lithologies, and their presence or absence cannot be predicted for modern subduction systems, so they

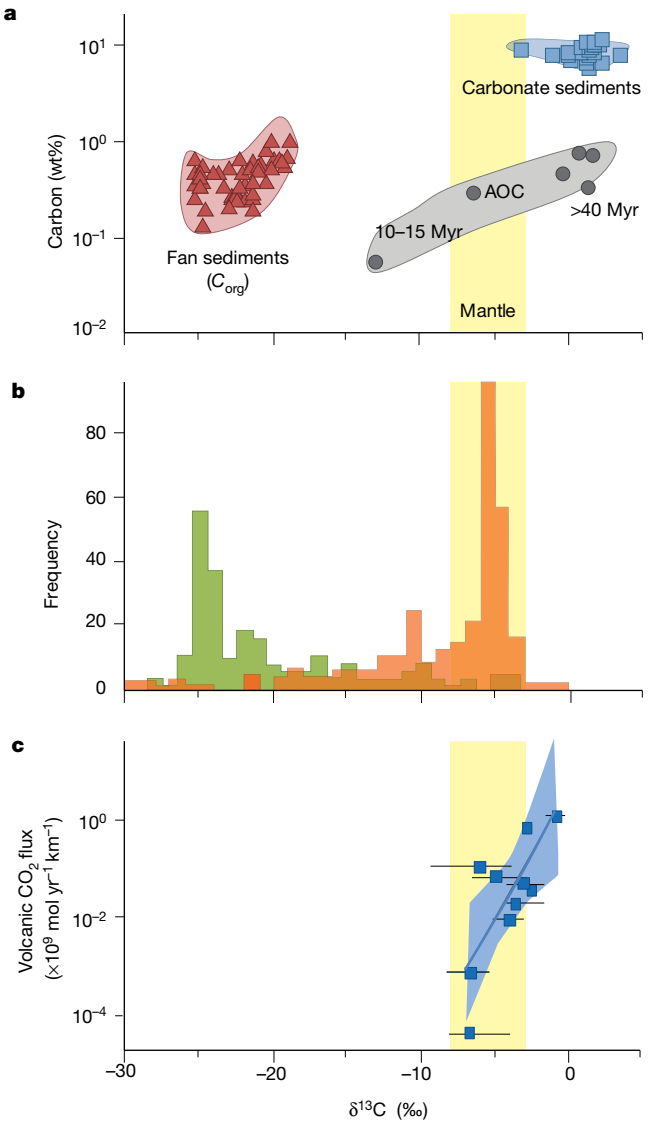

Fig. 2 | Carbon isotopes in subducted input, diamonds and arc volcanic gas. a, Subducted carbon input, including that in the upper volcanic layer of AOC older than 10 Myr (refs [30,102]), carbonate sediments from ODP site 765 (ref. [41]), total organic carbon, C_{org}, in Bengal Fan sediments[103]. **b**, Diamonds, including 319 eclogitic diamonds (orange; from ref. [30]) and Juina SLD (green; ref. [104]). **c**, Volcanic output per kilometre of arc from ref. [92], where error bars are one standard deviation about the mean value. Yellow shading encompasses mantle values. Diamond populations appear skewed towards light carbon isotopes[74], whereas arc volcanic C is skewed towards high $\delta^{13}C$ values[92]. It is unclear whether this reflects preferential recycling of carbonate to the arc and preferential subduction of more refractory organic carbon to the deeper mantle source of diamonds, or whether ancient diamonds reflect more-reduced sources in Earth's past[14].

are omitted here. Likewise, the extent of subduction erosion of forearc material is debated, as is its carbon content[34,42,43]. Mechanical removal reflects off-scraping and diapiric flow of large rock masses[44,45]. Because this is chiefly evident from past subduction complexes exhumed to the surface in the geologic record, only rarely is it possible to establish where and how mechanical removal operates today. A prominent instructive exception is in the Mariana forearc[46].

The removal of metamorphic carbon from the slab depends on the kindness of water. Carbonate minerals and graphite/diamond are stable on their own up to very high temperatures and pressures; in the absence of any other processes or materials, such carbon is extremely refractory and its recycling efficiency is low. However, subducted lithologies also carry hydrogen and oxygen bound in minerals, and the rising pressure and temperature drive their release to create a free aqueous fluid that is buoyant and reactive with carbon. The fluid strips carbon from these rocks, carries it along its path and deposits it downstream in rocks or melts as a response to changing conditions. Traditional thinking focused only on molecular forms of carbon in the fluid, such as CO_2, and concluded that its recycling efficiency is low, except perhaps in the hottest subduction systems[47–49]. Driven by emerging experimental and field studies, recent work also considers the roles of the oxidation state, pH and other rock constituents and dissolved species, generally leading to greater recycling efficiency[3,50–54]. Although carbon solubilities may contribute to substantial redistribution, they are probably insufficient on their own to account for the removal of all carbon in every instance.

The recycling efficiency can be substantially boosted by melting, especially at the slab top. Graphitized organic matter has very low solubility in sediment melts[14], and modern subduction geotherms yield temperatures that are typically too cool to trigger melting of subducted carbonate-bearing peridotite, AOC and sediment at sub-arc depths in the absence of a free water-rich fluid[55–57]. However, water-rich fluids, especially those sourced from dehydrating peridotites at sub-arc depths, can trigger melting, especially in the sedimentary layer. Melts derived from carbonate-bearing AOC and sediment can remove substantial carbon[58,59]. Moreover, in many subduction systems, the slab top beneath the arc is near conditions at which there is complete miscibility between sediment melt and aqueous fluid[60], making continuous dissolution the operative process. Such fluids have great transport capacity, although the role of carbon in them remains poorly understood. Carbonate-rich melts can be produced by the final stages of dehydration of subducted mantle lithosphere beneath the arc front[61].

Any carbon remaining after these processes may be transported in the slab or possibly in the superjacent mantle wedge[3]. At relatively shallow depths the overlying lithospheric mantle is static, but at a certain depth mantle wedge peridotite kinematically couples to the slab and is dragged downwards[62]. Thus, the downward-dragged mantle wedge represents an additional carbon sink created by the subduction process.

Much past debate focused on isolating a single mechanism as the primary pathway for carbon subtraction. Here we emphasize that it is more useful to recognize that several mechanisms can operate in parallel or in series, and that each global segment experiences them in unique proportion and extent. Considering the different carbon inputs to the global subduction system (Box 2), Box 3 describes the operation of the three distinct processing mechanisms for carbon removal. Metamorphic decarbonation is likely to operate in all subduction zones, although the extent to which this removes carbon varies with thermal structure and hydration extent. In the cold Tonga system, it is probably inefficient. The hot Cascadia subduction system stands in stark contrast, with substantial carbon loss by devolatilization/dissolution and melting of predominantly reduced sedimentary carbon. The Central American sediments, rich in biogenic carbon of both oxidized and reduced forms, may fractionate during devolatilization and melting, with preferential recycling of soluble, oxidized carbonate compared to less-soluble organic carbon. The slow-spreading crust feeding the South Sandwich system is expected to be dominated by carbonated peridotite in a young, warm slab. The degree to which mechanical diapiric transport operates today is not known; however, one setting in which it may have been important in the recent past could be the Alpine subduction system. Melting was unlikely as there was no volcanic arc. Though carbon inputs were likely high in Tethyan Mesozoic oceanic crust, the combination of diapirism and dissolution/dehydration could have driven substantial carbon recycling. These examples highlight the conspicuous expressions of individualism in Earth's subduction zones that become obscured by global averaging.

Carbon beyond the arc: diamonds and more

Carbon that survives beyond sub-arc depths is exceptionally challenging to investigate. In the absence of a fluid phase, even trace carbonate remaining in slab lithologies can trigger melting that may be small in volume but is geochemically important. Most slab geotherms will

Box 3

Carbon removal in the subduction zone

Each subducting system illustrates different mechanisms and recycling efficiencies. Tonga is cool, with little sediment but abundant oxidized carbon in mafic crust of Mesozoic age; the dominant carbon removal process is probably inefficient metamorphic decarbonation. Cascadia has higher temperature, and inputs include considerable amounts of reduced carbon. Combined metamorphic and melting processes probably achieve efficient carbon removal. In Central America there is subduction of substantial oxidized and reduced sedimentary carbon, in a young plate with low carbon concentration in the mafic crust. Geotherms lead to lower slab temperatures than those for Cascadia, but they are sufficient to yield metamorphic and melting loss of sedimentary C, with greater loss of carbonate than less-soluble organic carbon. South Sandwich is a subduction system in which inputs may be dominated by peridotitic carbonate. The Alpine system is shown for a speculative example in which mechanical removal may have been considerable, and carbon input was substantially higher in the Tethyan lithosphere.

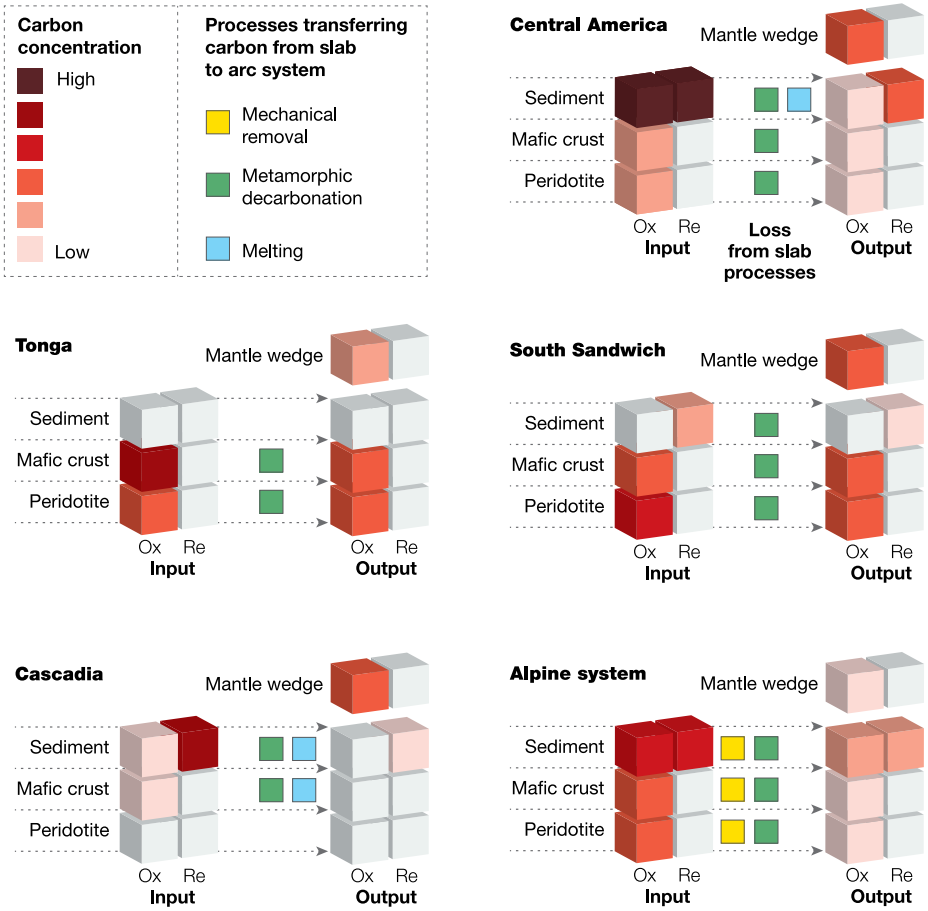

Box 3 Fig. 1 | Schematic representation of carbon inputs, outputs and removal in the global subduction system. The key (top left) shows vertically arrayed boxes representing lithospheric inputs and outputs in sediment, mafic crust and peridotite, partitioned between oxidized (Ox) and reduced (Re) carbon; outputs include carbon in the mantle wedge. Between the input and output columns are columns illustrating the processes transferring carbon from the slab to the arc system by mechanical removal, metamorphic decarbonation and melting. Examples from subduction segments (from Box 2) show inputs and outputs coloured as in the key in the box. White boxes indicate no carbon.

eventually intersect conditions at which carbonated crust melts[63,64], producing a magma highly enriched in carbonate known as carbonatite, which has extremely high mobility, very similar to that of water[65,66]. Such melts will quickly migrate into the surrounding mantle, where vastly different chemical conditions lead to reactions that transform carbon into new and more resistant forms such as diamond. The durability of diamond allows it to act as a long-term store of information about carbon mixing back into the mantle via subduction.

There are two geodynamically distinct reservoirs of subducted carbon in the mantle: the deep lithospheric keels beneath continents and the more voluminous, convecting upper mantle, transition zone and upper part of the lower mantle. Most diamonds are derived from the volumetrically minor lithosphere; relationships to subducted carbon exist but are difficult to quantify because of the complex history and great age of lithospheric diamonds. However, rare sub-lithospheric diamonds (SLD) appear to be more directly linked to deeper subduction processes extending into the transition zone and beyond. Study of these diamonds is transforming our understanding of the deep carbon cycle.

Key to the origin of SLD is the strong chemical contrast between the subducting crust and the ambient convecting mantle. This difference is not just in bulk composition but also, more importantly, in oxidation state. Whereas most crustal rocks are derived from Earth's oxidized

Box 4

Constraints on arc primary magmatic CO_2 concentrations and sources

Volcanic-arc gases have $CO_2/^3He$ and $\delta^{13}C$ ratios that are consistent with the mixing of three end-members: MORBs (reflecting background sub-arc mantle), marine carbonate and organic carbon (reflecting subducting sources)[108,109]. Provided that neither the isotopic nor the concentration ratios are fractionated, the proportion of the three end-members in the source carbon can be calculated from the mass balance. A recent compilation of high-temperature gases with minimal crustal contributions[110] found that 80–95% of arc carbon is recycled (Box 4 Fig. 1). This result derives entirely from the higher $CO_2/^3He$ ratios in arc versus MORB gases. Different C and He solubilities and diffusivities during degassing can fractionate this ratio[111], although in MORBs this leads to an average decrease of only 25% in the $CO_2/^3He$ ratio[107]. If the high arc $CO_2/^3He$ ratio reflected preferential He loss, then the arc CO_2/S ratio should also be lower than that of MORB (given the lower solubility of CO_2 versus S)—it is not[11]. Instead, the combined C–S–He systematics supports the conclusion that most of the CO_2 in arc magmas is recycled from the subduction zone, with the $\delta^{13}C$ value reflecting a predominance of carbonate sources.

Box 4 Table combines gas and magma data from two independent approaches and estimates ~1.2 wt% CO_2 in primary arc magmas and a CO_2 mole fraction of ~0.1 in the aggregate slab fluid/melt (assuming that all C is CO_2 and all H is H_2O). These quantities, here based on rough averages, have obvious power in testing different slab decarbonation scenarios. The way forward is to compare regional variations in $CO_2/^3He$, $\delta^{13}C$ and CO_2/S with different slab inputs (Box 2) and reaction models (Box 3) to quantify the efficiency of the deep carbon cycle.

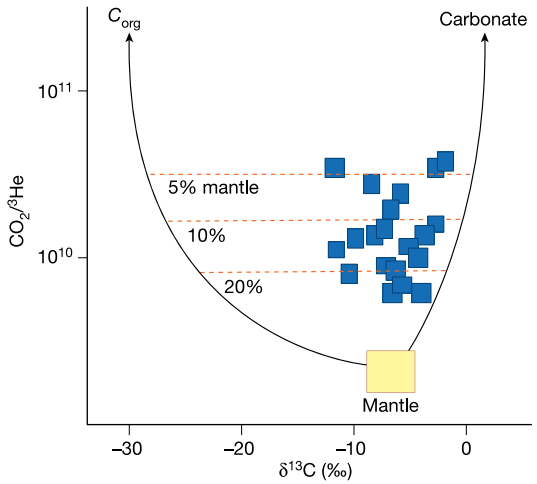

Box 4 Fig. 1 | C–He mixing relationships. Volcanic-arc gases (blue boxes) and mantle-subducting sediment mixing curves from ref. [108]. Dashed lines show the per cent contribution of the mantle end-member.

Box 4 Table | CO_2 in primary (initial, mantle-derived) arc magmas

Parameter	Value	Reference/calculation
1. Mantle CO_2/Nb	600	93
2. Arc Nb (ppm)	2	99
3. Arc CO_2 from mantle (ppm)	1,200	Line 1 × line 2
4. Mass fraction of mantle end-member in arc CO_2	0.1	Box 4 Fig. 1
5. Primary arc CO_2 (wt%)	1.2	Line 3/line 4
6. Arc gas CO_2/S	4	11
7. Arc magma S (ppm)	3,000	100
8. Primary arc CO_2 (wt%)	1.2	Line 6 × line 7
9. Arc magma H_2O (wt%)	4	101
10. H/C	1.4	Line 9/line 5
11. CO_2 mole fraction	0.11	From line 10

The table lists parameters, values and calculations used to derive estimates for the concentration of CO_2 in primary arc magmas. All quantities are expressed in mass units except line 11.

surface reservoirs, the mantle is relatively reducing, and becomes more so with depth. Driven chiefly by changes in the stability of iron-rich minerals with depth[67–71], this leads to conditions that stabilize an iron-rich metallic phase and, at depths greater than about 140 km, produce diamond as the stable form of carbon.

SLD are identified by virtue of the mineral inclusions that they hold, which signal a depth greater than that of the deepest lithospheric keels (>200 km). SLD are younger than lithospheric diamonds, show highly complex growth histories and display strong chemical links to subducted crust[72,73]. Carbon isotope data for SLD are quite variable, extending to very low $\delta^{13}C$ values consistent with carbon derivation from subducted sediment or altered basalt[30,72,74] (Fig. 2b).

If SLD are consistently associated with subducted carbon, then how do they form and how are they transported to the surface? The mineral inclusion assemblages in SLD may show peridotite affinity, but they dominantly host eclogitic mineral assemblages[75]. Traditionally, inclusion 'affinities' are assumed to identify the host rock in which diamond grew. This view implies a narrow set of rock types with a restricted range of chemical characteristics that make it difficult to explain the wide variations observed in SLD. However, an emerging alternative model posits that SLD and their inclusion phases coprecipitate from the fluids and melts derived from subducted crust, so that diamond and its inclusions are products of crystallization in the ambient mantle during reactive flow of melt migrating away from the slab. Low degrees of interaction yield coprecipitating phases that are more similar to the source eclogite, whereas higher degrees of interaction yield an assemblage that is more representative of the ambient mantle. Such a model predicts that inclusion assemblages are chemically linked although they appear to reflect different host rocks, and that there should be straightforward elemental and isotopic patterns consistent with the evolution of conditions from the eclogite source to the ambient mantle. This model better explains the highly enriched character of inclusion minerals, which are otherwise anomalous if they are direct samples of the slab[76]. It also explains C–O stable isotopic systematics[77].

SLD are but a small fraction of diamonds erupted in the kimberlites in which they are found, and diamond-bearing kimberlites are but a small fraction of all kimberlite magmas, which are themselves a minute but important component of global magmatism. As noted earlier, the vast majority of diamonds come from the subcontinental mantle lithosphere. Like SLD, they are best interpreted as metasomatic in origin, and some show evidence for the involvement of subducted carbon, but they differ from SLD in their great age (extending to more than 2.5 Gyr). A wide range of possible mechanisms form lithospheric diamonds, including mixing of mantle and subduction-related fluids,

precipitation from metallic melts and mechanical mixing of diamonds formed in subducted slabs with mantle before capture in the lithosphere. As with the happenstance of carbon subduction, the record of subducted carbon found in diamonds is also a highly random sample of material heterogeneously distributed in space and time; it is not in control of its own fate and it depends on largely independent processes to be mined from the deep.

Overall, the total amount of carbon that exists in the form of diamond is unknown. Even if kimberlite eruptions are taken as representative of normal mantle, the overall amount of carbon in diamond is small[3]. It seems likely that the more common return path for carbon stored in metal carbides and diamond is as a component of magmas derived from the mantle; it is typically so chemically modified that little can be said about the processes preceding melting.

Carbon returned: volcanic gas

Explosive volcanic eruptions—common within the volcanic arcs that form above subduction zones—are driven by the dramatic exsolution of volatiles, including CO_2, as magmas rise to the surface. This is due to a strong drop in solubility with decreasing pressure. Magmas can readily dissolve large quantities of carbon as carbonate in the mantle[78], but magmas with more than 1 wt% CO_2 will be vapour-saturated and degas throughout their entire ascent in the crust[79]. The standard method used to measure the concentration of magmatic volatiles is to analyse melt inclusions trapped in early-formed minerals. This approach has been successful in estimating the concentrations of H_2O, S, Cl and F, but not CO_2, owing to its much lower solubility at crustal pressures[80]. Moreover, as much as 90% of the CO_2 in a melt inclusion can be exsolved to a shrinkage bubble during cooling[81]. Unfortunately, the literature is replete with measurements of CO_2 in melt inclusions compromised by degassing or bubble formation. After bubble reconstruction, arc melt inclusions may contain thousands of parts per million of CO_2[82,83], but there is no guarantee that these melts did not lose CO_2 by degassing before inclusion formation. Thus, a major outstanding challenge is to determine the CO_2 concentration of primary arc magmas (Box 4).

Given that erupted magma has lost its CO_2, a more fruitful approach is to measure the lost gas. However, CO_2 above the atmospheric background is difficult to measure using remote-sensing techniques. Campaign-style gas measurements show large spatial and temporal variations in CO_2 fluxes in different volcanic systems including diffuse degassing from soils, springs and hydrothermal systems[84,85]. Diffuse degassing is generally strongest for large silicic calderas that erupt infrequently[10]. Thus, although satellite detection holds promise for the future[86], estimating CO_2 fluxes from volcanoes is difficult owing to its non-steady-state and non-point-source distribution.

A recent promising approach for the estimation of volcanic CO_2 fluxes has been to make use of the ratio of CO_2 to sulfur. Relatively inexpensive multicomponent gas analyser systems (such as Multi-GAS) have revolutionized our understanding of CO_2/S variations at different volcanoes over their eruption cycles. In addition to their great utility in eruption forecasting[87,88], multi-year records from persistently degassing volcanoes show that most gas release occurs passively during the inter-eruptive period[89]. Integrated CO_2/S correlates in some volcanic arcs with ratios of non-volatile trace elements (for example, Sr/Nd or Ba/La) linked to subduction recycling of carbonate and slab fluids[9]. Arcs with low CO_2/S ratio (for example, in the western Pacific) are associated with a lack of subducting sedimentary carbon, whereas those with higher CO_2/S ratios are associated with subducting sedimentary carbonate (Box 2). Sometimes magmas intercept limestones in the upper plate and drive decarbonation[90], a process recognized from an anomalously high CO_2/S ratio (>5) that is not linked to other slab tracers[89]. CO_2/S data have also led to CO_2 flux estimates[11] when coupled to volcanic SO_2 fluxes measured from space[7]. The biggest volcanic emitters are found where carbonate-rich sediments subduct (Central America, Vanuatu and Papua New Guinea), whereas low-CO_2-flux volcanoes occur where no carbonate sediments subduct (Kuriles-Aleutians; Box 2). These studies show clear signs that volcanic CO_2 variations reflect varying subducted input, but longer records are needed to understand temporal variations[91].

Another useful tool is C isotopic ratios in volcanic gases, which may be lower or higher than mantle values for individual volcanoes. Some gases have low $^3He/^4He$ ratios, a signal of upper-crustal contamination[92]; however, the full range of $\delta^{13}C$ values is found in volcanic gases that have mantle-like $^3He/^4He$. Low-$\delta^{13}C$ volcanic carbon occurs at margins where low-$\delta^{13}C$ organic carbon is subducted (for example, the Aleutians), whereas high $\delta^{13}C$ values occur where high-$\delta^{13}C$ carbonate is subducted (for example, Central America; Box 2). Globally, volcanic arcs with the highest C fluxes have the highest $\delta^{13}C$, suggesting a dominance of carbonate sources (Fig. 2c). This could reflect preferential recycling of carbonate in the subduction zone. The $CO_2/^3He$ ratios of arc volcanic gases are consistent with most of the carbon (80–95%) being derived from recycled, subducted sources (Box 4). These constraints, coupled with those from the CO_2/S and CO_2/Nb ratios, point to primary arc magmas containing up to 1 wt% CO_2 (Box 4), an order of magnitude higher than that of average mid-ocean-ridge basalt (MORB; about 1,000 ppm)[93]. Volcanic-arc data are still sparse, however, and portable mass spectrometers mounted on helicopters[94] and field vehicles[95] are providing new methods for carbon isotope analysis in remote regions. Carbon isotope measurements in springs are also revealing subducting and upper-plate sources, as well as sequestration in the biosphere[96].

Conclusions

Carbon subduction is neither a steady-state nor a globally averaged process. The input fluxes to deep sea trenches are spatially and temporally heterogeneous, as are slab pressure–temperature paths, and thus every subduction zone is a different carbon recycling experiment. In this Review, we have developed three essential viewpoints:

(1) Carbon subduction is geological happenstance. Fixing carbon in oceanic peridotite or burying it in sediments is inherently difficult, as the long path lengths and high solubilities in the deep ocean work against it. Sedimentary carbon is virtually absent from some subduction zones and dominates others (Box 2). Carbonate veining is pervasive in the oceanic crust but its extent varies with crustal age (Fig. 2a). Past (Tethys subduction) or future (Atlantic subduction) carbonate inputs might be larger than those occurring today. At other times, continent collision and erosion deliver organic carbon to deep-sea fans that subduct. Such tectonic events will affect the climate system over long timescales.

(2) Sediments drive the variability in subducting carbon. If the latest flux estimates are accurate (Box 1), then carbonate sediments dominate the subducting flux of carbon by a factor of about two over oceanic-crust and peridotite input fluxes. Recycling of carbonate may explain the high C fluxes and high $\delta^{13}C$ values observed in some volcanic arcs (Fig. 2c). Sediments also supply the greatest flux of organic carbon to the solid Earth (Box 1), and the fate of reduced and isotopically light carbon is critical to the oxidation state of Earth's surface and mantle, and may relate to the low $\delta^{13}C$ values of eclogitic diamonds (Fig. 2b). There may be a complementarity to C isotopes, with heavy carbon isotopes reflecting predominantly carbonate recycling beneath arcs and light carbon isotopes representing deep subduction of organic carbon as a source of diamonds.

(3) There is no single recycling efficiency for carbon. The recycling of carbon back to Earth's surface via arc volcanism depends on the carbon-carrying capacity of fluids and melts in each subduction zone, which in turn are a function of the slab pressure–temperature paths, the pH and redox potentials, and the bulk compositions of each system (Box 3). Not only does the input vary for each subduction zone, but so also do the parameters that govern the recycling efficiency. Current global flux balances (Box 1) place carbon recycling efficiency at 25%, but the associated uncertainties are very large. Even if accurate, this number is insufficiently precise, so the global average carries questionable meaning for any particular margin, and its variation with time

could be substantial. For example, carbonate recycling could be more efficient than organic carbon recycling, and sedimentary carbon could be more easily liberated than oceanic-crust carbon. Modern subduction zones offer many natural experimental settings (Box 2) to test how initial conditions, such as plate age and organic-to-inorganic ratio, affect recycling efficiency (Box 3). Carbon–helium–sulfur systematics point to 80–95% of arc volcanic carbon deriving from the subduction zone (Box 4), so the signal is large. The stakes are high for the climate system, with subducting carbon acting as a source or sink, depending on its recycling efficiency. Coordinated effort is needed on all fronts—quantifying carbon inputs, modelling chemical transfer in the subduction zone and measuring volcanic outputs and deep diamonds—to constrain the global impacts of subducting carbon.

Received: 17 June 2019; Accepted: 11 September 2019;
Published online 16 October 2019.

1. Hayes, J. M. & Waldbauer, J. R. The carbon cycle and associated redox processes through time. *Philos. Trans. R. Soc. Lond. B* **361**, 931–950 (2006).
2. Dasgupta, R. & Hirschmann, M. M. The deep carbon cycle and melting in Earth's interior. *Earth Planet. Sci. Lett.* **298**, 1–13 (2010).
This article examines the global carbon budget and the mobility of carbon in the mantle.
3. Kelemen, P. B. & Manning, C. E. Reevaluating carbon fluxes in subduction zones, what goes down, mostly comes up. *Proc. Natl Acad. Sci. USA* **112**, E3997–E4006 (2015).
This review summarizes carbon inputs and outputs to the mantle and emphasizes the potential for carbon to be efficiently recycled from the slab and potentially stored in the arc lithosphere.
4. Hirschmann, M. M. Comparative deep Earth volatile cycles: the case for C recycling from exosphere/mantle fractionation of major (H_2O, C, N) volatiles and from H_2O/Ce, CO_2/Ba, and CO_2/Nb exosphere ratios. *Earth Planet. Sci. Lett.* **502**, 262–273 (2018).
This paper sets carbon recycling in the context of other volatile components.
5. Galvez, M. E. & Pubellier, M. in *Deep Carbon: Past to Present* (eds Orcutt, B. N. et al.) 276–309 (Cambridge Univ. Press, 2019).
6. Lee, C. T. A., Jiang, H., Dasgupta, R. & Torres, M. in *Deep Carbon: Past to Present* (eds Orcutt, B. N. et al.) 313–357 (Cambridge Univ. Press, 2019).
7. Carn, S. A., Fioletov, V. E., McLinden, C. A., Li, C. & Krotkov, N. A. A decade of global volcanic SO_2 emissions measured from space. *Sci. Rep.* **7**, 44095 (2017).
8. Burton, M. R., Sawyer, G. M. & Granieri, D. Deep carbon emissions from volcanoes. *Rev. Mineral. Geochem.* **75**, 323–354 (2013).
9. Aiuppa, A. et al. Gas measurements from the Costa Rica–Nicaragua volcanic segment suggest possible along-arc variations in volcanic gas chemistry. *Earth Planet. Sci. Lett.* **407**, 134–147 (2014).
10. Werner, C. et al. in *Deep Carbon: Past to Present* (eds Orcutt, B. N. et al.) 188–236 (Cambridge Univ. Press, 2019).
11. Aiuppa, A., Fischer, T. P., Plank, T. & Bani, P. CO_2 flux emissions from the Earth's most actively degassing volcanoes, 2005–2015. *Sci. Rep.* **9**, 5442 (2019).
12. Friedlingstein, P. et al. Update on CO_2 emissions. *Nat. Geosci.* **3**, 811–812 (2010).
13. Hirschmann, M. M. & Dasgupta, R. The H/C ratios of Earth's near-surface and deep reservoirs and consequences for deep Earth volatile cycles. *Chem. Geol.* **262**, 4–16 (2009).
14. Duncan, M. S. & Dasgupta, R. Rise of Earth's atmospheric oxygen controlled by efficient subduction of organic carbon. *Nat. Geosci.* **10**, 387–392 (2017).
15. Evans, K. A. The redox budget of subduction zones. *Earth Sci. Rev.* **113**, 11–32 (2012).
16. Edmond, J. M. & Huh, Y. Non-steady state carbonate recycling and implications for the evolution of atmospheric PCO_2. *Earth Planet. Sci. Lett.* **216**, 125–139 (2003).
17. Kent, D. V. & Muttoni, G. Modulation of Late Cretaceous and Cenozoic climate by variable drawdown of atmospheric pCO_2 from weathering of basaltic provinces on continents drifting through the equatorial humid belt. *Clim. Past* **9**, 525–546 (2013).
18. Krissansen-Totton, J. & Catling, D. C. Constraining climate sensitivity and continental versus seafloor weathering using an inverse geological carbon cycle model. *Nat. Commun.* **8**, 15423 (2017).
19. Müller, R. D., & Dutkiewicz, A. Oceanic crustal carbon cycle drives 26-million-year atmospheric carbon dioxide periodicities. *Sci Adv.* **4**, eaaq0500 (2018).
20. Volk, T. Sensitivity of climate and atmospheric CO_2 to deep-ocean and shallow-ocean carbonate burial. *Nature* **337**, 637–640 (1989).
21. Johnston, F. K., Turchyn, A. V. & Edmonds, M. Decarbonation efficiency in subduction zones: implications for warm Cretaceous climates. *Earth Planet. Sci. Lett.* **303**, 143–152 (2011).
22. Kelemen, P. B. et al. Rates and mechanisms of mineral carbonation in peridotite: natural processes and recipes for enhanced, in situ CO_2 capture and storage. *Annu. Rev. Earth Planet. Sci.* **39**, 545–576 (2011).
23. Alt, J. C. et al. The role of serpentinites in cycling of carbon and sulfur: seafloor serpentinization and subduction metamorphism. *Lithos* **178**, 40–54 (2013).
This review describes the carbon cycle driven by serpentinization and subduction.
24. Tonarini, S., Leeman, W. P. & Leat, P. T. Subduction erosion of forearc mantle wedge implicated in the genesis of the South Sandwich Island (SSI) arc: evidence from boron isotope systematics. *Earth Planet. Sci. Lett.* **301**, 275–284 (2011).
25. Grevemeyer, I., Ranero, C. R. & Ivandic, M. Structure of oceanic crust and serpentinization at subduction trenches. *Geosphere* **14**, 395–418 (2018).
26. Parai, R. & Mukhopadhyay, S. How large is the subducted water flux? New constraints on mantle regassing rates. *Earth Planet. Sci. Lett.* **317–318**, 396–406 (2012).
27. Cai, C., Wiens, D. A., Shen, W. & Eimer, M. Water input into the Mariana subduction zone estimated from ocean-bottom seismic data. *Nature* **563**, 389 (2018).
28. Naif, S., Key, K., Constable, S. & Evans, R. L. Water-rich bending faults at the Middle America Trench. *Geochem. Geophys. Geosyst.* **16**, 2582–2597 (2015).
29. Shilobreeva, S., Martinez, I., Busigny, V., Agrinier, P. & Laverne, C. Insights into C and H storage in the altered oceanic crust: results from ODP/IODP Hole 1256D. *Geochim. Cosmochim. Acta* **75**, 2237–2255 (2011).
30. Li, K., Li, L., Pearson, D. G. & Stachel, T. Diamond isotope compositions indicate altered igneous oceanic crust dominates deep carbon recycling. *Earth Planet. Sci. Lett.* **516**, 190–201 (2019).
This paper provides recent data on the carbon content and isotopic composition of AOC and considers the subducted flux and its contribution to diamonds.
31. Alt, J. C. & Teagle, D. A. H. The uptake of carbon during alteration of ocean crust. *Geochim. Cosmochim. Acta* **63**, 1527–1535 (1999).
32. Gillis, K. M. & Coogan, L. A. Secular variation in carbon uptake into the ocean crust. *Earth Planet. Sci. Lett.* **302**, 385–392 (2011).
33. Hayes, J. M., Strauss, H. & Kaufman, A. J. The abundance of ^{13}C in marine organic matter and isotopic fractionation in the global biogeochemical cycle of carbon during the past 800 Ma. *Chem. Geol.* **161**, 103–125 (1999).
34. Clift, P. D. A revised budget for Cenozoic sedimentary carbon subduction. *Rev. Geophys.* **55**, 97–125 (2017).
35. Pälike, H. et al. A Cenozoic record of the equatorial Pacific carbonate compensation depth. *Nature* **488**, 609 (2012).
36. Van Andel, T. H. Mesozoic/Cenozoic calcite compensation depth and the global distribution of calcareous sediments. *Earth Planet. Sci. Lett.* **26**, 187–194 (1975).
37. Syracuse, E. M. & Abers, G. A. Global compilation of variations in slab depth beneath arc volcanoes and implications. *Geochem. Geophys. Geosyst.* **7**, Q05017 (2006).
38. Plank, T. in *Treatise on Geochemistry* 2nd edn, Vol. 4 (eds Holland, H. D. & Turekian, K. K.) 607–629 (Elsevier, 2014).
39. Galy, V. et al. Efficient organic carbon burial in the Bengal fan sustained by the Himalayan erosional system. *Nature* **450**, 407–410 (2007).
40. D'Hondt, S. et al. Presence of oxygen and aerobic communities from sea floor to basement in deep-sea sediments. *Nat. Geosci.* **8**, 299–304 (2015).
41. House, B. M., Bebout, G. E. & Hilton, D. R. Carbon cycling at the Sunda margin, Indonesia: a regional study with global implications. *Geology* **47**, 483–486 (2019).
42. Regalla, C., Fisher, D. M., Kirby, E. & Furlong, K. P. Relationship between outer forearc subsidence and plate boundary kinematics along the Northeast Japan convergent margin. *Geochem. Geophys. Geosyst.* **14**, 5227–5243 (2013).
43. Freundt, A. et al. Volatile (H_2O, CO_2, Cl, S) budget of the Central American subduction zone. *Int. J. Earth Sci.* **103**, 2101–2127 (2014).
44. Gerya, T. V., Stoeckhert, B. & Perchuk, A. L. Exhumation of high-pressure metamorphic rocks in a subduction channel – a numerical simulation. *Tectonics* **21**, 1056 (2002).
45. Gerya, T. V. & Meilick, F. I. Geodynamic regimes of subduction under an active margin: effects of rheological weakening by fluids and melts. *J. Metamorph. Geol.* **29**, 7–31 (2011).
46. Fryer, P., Ambos, E. L. & Hussong, D. M. Origin and emplacement of Mariana forearc seamounts. *Geology* **13**, 774–777 (1985).
47. Kerrick, D. M. & Connolly, J. A. D. Metamorphic devolatilization of subducted marine sediments and the transport of volatiles into the Earth's mantle. *Nature* **411**, 293 (2001).
48. Kerrick, D. M. & Connolly, J. A. D. Metamorphic devolatilization of subducted oceanic metabasalts: implications for seismicity, arc magmatism and volatile recycling. *Earth Planet. Sci. Lett.* **189**, 19–29 (2001).
49. Gorman, P. J., Kerrick, D. M. & Connolly, J. A. D. Modeling open system metamorphic decarbonation of subducting slabs. *Geochem. Geophys. Geosyst.* **7**, Q04007 (2006).
50. Ague, J. J. & Nicolescu, S. Carbon dioxide released from subduction zones by fluid-mediated reactions. *Nat. Geosci.* **7**, 355–360 (2014).
This paper provides evidence for carbon transport in subduction zone fluids by dissolution of $CaCO_3$ versus metamorphic decarbonation.
51. Galvez, M. E., Connolly, J. A. D. & Manning, C. E. Implications for metal and volatile cycles from the pH of subduction zone fluids. *Nature* **539**, 420–424 (2016).
52. Galvez, M. E., Manning, C. E., Connolly, J. A. D. & Rumble, D. The solubility of rocks in metamorphic fluids: a model for rock-dominated conditions to upper mantle pressure and temperature. *Earth Planet. Sci. Lett.* **430**, 486–498 (2015).
53. Gorce, J. S., Caddick, M. J. & Bodnar, R. J. Thermodynamic constraints on carbonate stability and carbon volatility during subduction. *Earth Planet. Sci. Lett.* **519**, 213–222 (2019).
54. Sverjensky, D. A. & Huang, F. Diamond formation due to a pH drop during fluid–rock interactions. *Nat. Commun.* **6**, 8702 (2015).

55. Tsuno, K. & Dasgupta, R. Melting phase relation of nominally anhydrous, carbonated pelitic-eclogite at 2.5–3.0 GPa and deep cycling of sedimentary carbon. *Contrib. Mineral. Petrol.* **161**, 743–763 (2011).
56. Dasgupta, R., Hirschmann, M. M. & Withers, A. C. Deep global cycling of carbon constrained by the solidus of anhydrous, carbonated eclogite under upper mantle conditions. *Earth Planet. Sci. Lett.* **227**, 73–85 (2004).
57. Hammouda, T. & Keshav, S. Melting in the mantle in the presence of carbon: review of experiments and discussion on the origin of carbonatites. *Chem. Geol.* **418**, 171–188 (2015).
58. Grassi, D. & Schmidt, M. W. The melting of carbonated pelites from 70 to 700 km depth. *J. Petrol.* **52**, 765–789 (2011).
59. Martin, L. A. & Hermann, J. Experimental phase relations in altered oceanic crust: implications for carbon recycling at subduction zones. *J. Petrol.* **59**, 299–320 (2018).
60. Cooper, L. B. et al. Global variations in H_2O/Ce: 1. Slab surface temperatures beneath volcanic arcs. *Geochem. Geophys. Geosyst.* **13**, Q03024 (2012).
61. Poli, S. Carbon mobilized at shallow depths in subduction zones by carbonatitic liquids. *Nat. Geosci.* **8**, 633–636 (2015).
62. van Keken, P. E., Kiefer, B. & Peacock, S. M. High resolution models of subduction zones: implications for mineral dehydration reactions and the transport of water into the deep mantle. *Geochem. Geophys. Geosyst.* **3**, 1056 (2002).
63. Thomson, A. R., Walter, M. J., Kohn, S. C. & Brooker, R. A. Slab melting as a barrier to deep carbon subduction. *Nature* **529**, 76–79 (2016).
This paper presents new results on slab melting below the mantle transition zone, which support a new reaction–transport model of sub-lithospheric diamond formation.
64. Sun, C. & Dasgupta, R. Slab–mantle interaction, carbon transport, and kimberlite generation in the deep upper mantle. *Earth Planet. Sci. Lett.* **506**, 38–52 (2019).
65. Kono, Y. et al. Ultralow viscosity of carbonate melts at high pressures. *Nat. Commun.* **5**, 5091 (2014).
66. Stagno, V. et al. in *Carbon in Earth* (eds Manning, C. E. et al.) (American Geophysical Union, 2019).
67. O'Neill, H. S. C., Rubie, D. C., Canil, D., Geiger, C. & Ross, C. R. in *Evolution of the Earth and Planets* Vol. 74 (eds Takahashi, E. et al.) 73–88 (American Geophysical Union, Washington, 1993).
68. Rohrbach, A. et al. Metal saturation in the upper mantle. *Nature* **449**, 456–458 (2007).
69. Frost, D. J. et al. Experimental evidence for the existence of iron-rich metal in Earth's lower mantle. *Nature* **428**, 409–412 (2004).
70. Frost, D. J. & McCammon, C. A. The redox state of Earth's mantle. *Annu. Rev. Earth Planet. Sci.* **36**, 389–420 (2008).
71. Ballhaus, C. Is the upper mantle metal-saturated? Earth Planet. *Sci. Lett.* **132**, 75–86 (1995).
72. Shirey, S. B. et al. Diamonds and the geology of mantle carbon. *Rev. Mineral. Geochem.* **75**, 355–421 (2013).
73. Smith, E. M. et al. Blue boron-bearing diamonds from Earth's lower mantle. *Nature* **560**, 84 (2018).
74. Cartigny, P. Stable isotopes and the origin of diamond. *Elements* **1**, 79–84 (2005).
75. Shirey, S. B. et al. Diamonds and the mantle geodynamics of carbon: deep mantle carbon evolution from the diamond record. In *Deep Carbon: Past to Present* (eds Orcutt, B. N. et al.) 89–128 (Cambridge Univ. Press, 2019).
This review provides the most up-to-date information on diamond formation and links to subduction.
76. Thomson, A. R. et al. Trace element composition of silicate inclusions in sub-lithospheric diamonds from the Juina-5 kimberlite: evidence for diamond growth from slab melts. *Lithos* **265**, 108–124 (2016b).
77. Burnham, A. D. et al. Stable isotope evidence for crustal recycling as recorded by superdeep diamonds. *Earth Planet. Sci. Lett.* **432**, 374–380 (2015).
78. Dasgupta, R. et al. Carbon-dioxide-rich silicate melt in the Earth's upper mantle. *Nature* **493**, 211–215 (2013).
79. Wallace, P. J. Volatiles in subduction zone magmas: concentrations and fluxes based on melt inclusion and volcanic gas data. *J. Volcanol. Geotherm. Res.* **140**, 217–240 (2005).
80. Wallace, P., Plank, T., Edmonds, M. & Hauri, E. H. in *The Encyclopedia of Volcanoes* 2nd edn Vol. I (eds. Sigurdsson H.) 163–183 (Elsevier, 2015).
81. Moore, L. R. et al. Bubbles matter: an assessment of the contribution of vapor bubbles to melt inclusion volatile budgets. *Am. Mineral.* **100**, 806–823 (2015).
82. Mironov, N. et al. Quantification of the CO_2 budget and H_2O–CO_2 systematics in subduction-zone magmas through the experimental hydration of melt inclusions in olivine at high H_2O pressure. *Earth Planet. Sci. Lett.* **425**, 1–11 (2015).
83. Aster, E. M. et al. Reconstructing CO_2 concentrations in basaltic melt inclusions using Raman analysis of vapor bubbles. *J. Volcanol. Geotherm. Res.* **323**, 148–162 (2016).
84. James, E. R., Manga, M. & Rose, T. P. CO_2 degassing in the Oregon Cascades. *Geology* **27**, 823–826 (1999).
85. Chiodini, G. et al. Carbon dioxide diffuse degassing and estimation of heat release from volcanic and hydrothermal systems. *J. Geophys. Res.* **110**, B08204 (2005).
86. Schwandner, F. M. et al. Spaceborne detection of localized carbon dioxide sources. *Science* **358**, eaam5782 (2017).
87. Aiuppa, A. et al. Patterns in the recent 2007–2008 activity of Mount Etna volcano investigated by integrated geophysical and geochemical observations. *Geochem. Geophys. Geosyst.* **11**, Q09008 (2010).
88. de Moor, J. M. et al. Turmoil at Turrialba Volcano (Costa Rica): degassing and eruptive processes inferred from high-frequency gas monitoring. *J. Geophys. Res.* **121**, 5761–5775 (2016).
89. Aiuppa, A., Fischer, T. P., Plank, T., Robidoux, P. & Di Napoli, R. Along-arc, inter-arc and arc-to-arc variations in volcanic gas CO_2/S_T ratios reveal dual source of carbon in arc volcanism. *Earth Sci. Rev.* **168**, 24–47 (2017).
This paper provides an example of the potential power of MultiGas data from volcanic vents to constrain CO_2 sources in the subduction zone.
90. Lee, C.-T. A. et al. Continental arc–island arc fluctuations, growth of crustal carbonates, and long-term climate change. *Geosphere* **9**, 21–36 (2013).
91. de Moor, J. M. et al. A new sulfur and carbon degassing inventory for the Southern Central American Volcanic Arc: the importance of accurate time-series data sets and possible tectonic processes responsible for temporal variations in arc-scale volatile emissions. *Geochem. Geophys. Geosyst.* **18**, 4437–4468 (2017).
92. Mason, E., Edmonds, M. & Turchyn, A. V. Remobilization of crustal carbon may dominate volcanic arc emissions. *Science* **357**, 290–294 (2017).
This paper reviews carbon isotopic compositions for volcanic gases globally and discusses crustal versus subducted sources of volcanic carbon and the implications for the carbon cycle.
93. Le Voyer, M. et al. Carbon fluxes and primary magma CO_2 contents along the global mid-ocean ridge system. *Geochem. Geophys. Geosyst.* **20**, 1387–1424 (2019).
94. Fischer, T. P. & Lopez, T. M. First airborne samples of a volcanic plume for $\delta^{13}C$ of CO_2 determinations. *Geophys. Res. Lett.* **43**, 3272–3279 (2016).
95. Rizzo, A. L. et al. Real-time measurements of the concentration and isotope composition of atmospheric and volcanic CO_2 at Mount Etna (Italy). *Geophys. Res. Lett.* **41**, 2382–2389 (2014).
96. Barry, P. H. et al. Forearc carbon sink reduces long-term volatile recycling into the mantle. *Nature* **568**, 487–492 (2019); correction **568**, E7 (2019).
97. Lawver, L. A. & Dick, H. J. The American-Antarctic Ridge. *J. Geophys. Res.* **88**, 8193–8202 (1983).
98. Syracuse, E. M., van Keken, P. E. & Abers, G. A. The global range of subduction zone thermal models. *Phys. Earth Planet. Inter.* **183**, 73–90 (2010).
99. Turner, S. J. & Langmuir, C. H. What processes control the chemical compositions of arc front stratovolcanoes? Geochem. *Geophys. Geosyst.* **16**, 1865–1893 (2015).
100. Zimmer, M. M. et al. The role of water in generating the calc-alkaline trend: new volatile data for Aleutian magmas and a new tholeiitic index. *J. Petrol.* **51**, 2411–2444 (2010).
101. Plank, T., Kelley, K. A., Zimmer, M. M., Hauri, E. H. & Wallace, P. J. Why do mafic arc magmas contain ~4 wt% water on average? *Earth Planet. Sci. Lett.* **364**, 168–179 (2013).
102. Alt, J. C. Stable isotopic composition of upper oceanic crust formed at a fast spreading ridge, ODP Site 801. *Geochem. Geophys. Geosyst.* **4**, 8908 (2003).
103. Galy, V., France-Lanord, C., Peucker-Ehrenbrink, B. & Huyghe, P. Sr–Nd–Os evidence for a stable erosion regime in the Himalaya during the past 12 Myr. *Earth Planet. Sci. Lett.* **290**, 474–480 (2010).
104. Thomson, A. R. et al. Origin of sub-lithospheric diamonds from the Juina-5 kimberlite (Brazil): constraints from carbon isotopes and inclusion compositions. *Contrib. Mineral. Petrol.* **168**, 1081 (2014).
105. Jarrard, R. D. Subduction fluxes of water, carbon dioxide, chlorine, and potassium. *Geochem. Geophys. Geosyst.* **4**, 8905 (2003).
106. Dutkiewicz, A., Müller, R. D., Cannon, J., Vaughan, S. & Zahirovic, S. Sequestration and subduction of deep-sea carbonate in the global ocean since the Early Cretaceous. *Geology* **47**, 91–94 (2018).
107. Tucker, J. M., Mukhopadhyay, S. & Gonnermann, H. M. Reconstructing mantle carbon and noble gas contents from degassed mid-ocean ridge basalts. *Earth Planet. Sci. Lett.* **496**, 108–119 (2018).
108. Sano, Y. & Marty, B. Origin of carbon in fumarolic gas from island arcs. *Chem. Geol.* **119**, 265–274 (1995).
109. Hilton, D. R., Fischer, T. P. & Marty, B. Noble gases and volatile recycling at subduction zones. *Rev. Mineral. Geochem.* **47**, 319–370 (2002).
110. Kagoshima, T. et al. Sulphur geodynamic cycle. *Sci. Rep.* **5**, 8330 (2015).
111. Gonnermann, H. M. & Mukhopadhyay, S. Non-equilibrium degassing and a primordial source for helium in ocean-island volcanism. *Nature* **449**, 1037–1040 (2007).

Acknowledgements This work was supported by the Deep Carbon Observatory. We thank the late E. Hauri, whose leadership and vision put into motion much of the research on carbon reservoirs and fluxes and on volcanic gas and magma chemistry reported here. We thank A. Malinverno, A. Thomson, S. Shirey, O. Tschauener, M. Walter, A. Aiuppa, T. Fischer, E. Cottrell and D. Kent for discussions, and J. M. de Moor and D. Muller for their comments.

Author contributions Both T.P. and C.E.M. contributed to the structure, content and message of this review.

Competing interests The authors declare no competing interests.

Additional information
Reprints and permissions information is available at http://www.nature.com/reprints.
Correspondence and requests for materials should be addressed to T.P.
Peer review information *Nature* thanks J. Maarten de Moor, Dietmar Muller and the other, anonymous, reviewer(s) for their contribution to the peer review of this work.
Publisher's note Springer Nature remains neutral with regard to jurisdictional claims in published maps and institutional affiliations.